

NON-PERTURBATIVE STRUCTURE OF THE NUCLEON

A. W. THOMAS

*Department of Physics and Mathematical Physics,
and Special Research Centre for the Subatomic Structure of Matter,
University of Adelaide,
Adelaide, 5005 Australia
E-mail: athomas@physics.adelaide.edu.au*

While much attention has been focussed on the successes of perturbative QCD in describing the Q^2 -dependence of deep-inelastic structure functions, the starting distributions themselves contain important, non-perturbative information on the structure of the nucleon, which has been somewhat neglected. We review some of the most important, recent discoveries resulting from studies of deep-inelastic scattering. There are important connections between these discoveries and low energy properties of the nucleon and wherever possible we shall make these clear. In particular, we shall see that well known features of QCD, such as dynamical symmetry breaking, are reflected in the properties of the measured parton distributions.

1 Introduction

There have recently been some very promising advances in lattice QCD as a result of the development of improved actions¹. In addition, we have a wealth of sophisticated models of hadron structure built on our knowledge of QCD, especially its symmetries. While lattice QCD cannot yet compete with such models in certain critical areas of hadron structure, such as dynamical symmetry breaking, all theoretical approaches can benefit from precise experimental insights into the problem. Apart from the usual low energy properties, such as masses, charge radii and magnetic moments, there is a wealth of information available from deep-inelastic scattering which is just beginning to be taken seriously as a source of information on non-perturbative physics².

We shall review the latest experimental information on the light-quark sea of the nucleon, which shows a dramatic deviation from the naive expectations of perturbative QCD. From this starting point it is natural to ask about the strange and even the charm components of the sea of the nucleon. These components will be the focus of considerable investigation in the near future. From the sea we turn to the behaviour of the valence quark distributions and particularly the behaviour of the distributions at large- x . Here too there are a number of surprises from the most recent analysis of the experimental data and, in the case of spin-dependent distributions, some interesting ideas to be tested.

2 $SU(2)_F$ Violation

The fundamental degrees of freedom in QCD are quarks and gluons, and for a considerable time there was great reluctance to include any other degrees of freedom in modeling hadron structure. On the other hand, extensive studies of non-perturbative QCD have shown that the chiral symmetry of the QCD Lagrangian is dynamically broken and that the resulting, massive constituent quarks must be coupled to pions. As pseudo-Goldstone bosons, the latter would be massless in the chiral limit. Most importantly, as emphasised by extensive work on chiral perturbation theory, *no perturbative treatment of $q\bar{q}$ creation and annihilation can ever generate the non-analytic behaviour in the light quark mass for physical quantities (such as $M, \langle r^2 \rangle, \sigma_{\pi N}$) which are generated by these Goldstone bosons*. As a consequence, it is now difficult to imagine a realistic quark model which does not incorporate at least the pion cloud of the nucleon.

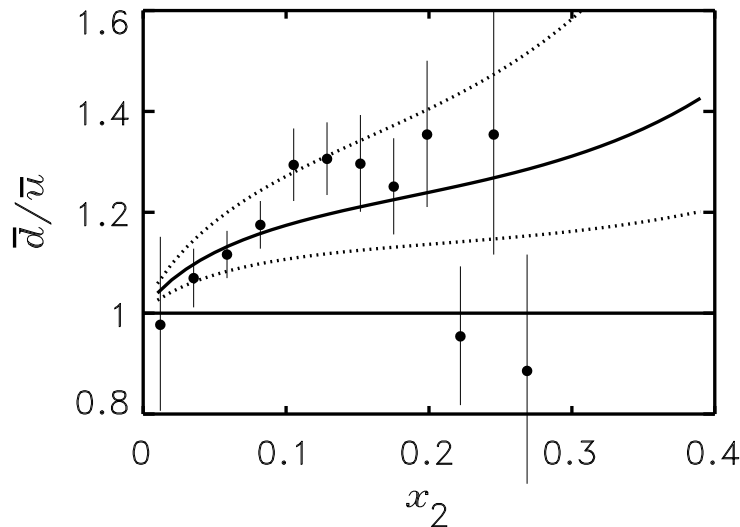


Figure 1: Comparison of the value of \bar{d}/\bar{u} extracted from the recent E866 data³ with the expectations from just the πN Fock component of the nucleon wave function, for three different form factors at the πN vertex – from Ref. ⁴.

The development of chiral quark models began in the late 1970's^{5,6,7,8} and

it became clear that the pion field had very important practical consequences for the low energy properties of hadrons. For example, the coupling to a “bare” nucleon lowers its mass by several hundred MeV, and can contribute a large part of the $N - \Delta$ mass difference, while the charge form factor of the neutron is a first order effect of its pion cloud⁸.

However, the relevance of the pion cloud for deep inelastic scattering, which had been first realized by Sullivan⁹, was not explored in depth until the discovery of the nuclear EMC effect, when it was suggested that the effect might be caused by a nuclear enhancement of the pion field of the bound nucleons^{10,11}. At this time it was realized that the light mass of the pion would lead to an enhancement of the non-strange over the strange sea of the nucleon¹², and this was used to put a constraint on the pion-nucleon form factor — a limit that has since been explored in detail¹³. A more important consequence of the nucleon’s pion cloud, which was also pointed out in Ref.¹², was an excess of \bar{d} over \bar{u} quarks. In particular, simple Clebsch-Gordan coefficients for isospin show that the pion cloud of the proton is in the ratio 2:1 for $\pi^+ : \pi^0$. Since the π^+ contains only a valence \bar{d} and the π^0 equal amounts of \bar{d} and \bar{u} , this component of the pion cloud of the nucleon yields a ratio for $\bar{d} : \bar{u}$ of 5:1.

On the other hand, perturbative QCD inevitably leads to the conclusion that $\bar{u} = \bar{d}$, a result known as SU(2)-flavor, SU(2)_F, symmetry. The latter is a very misleading name as there is *no rigorous symmetry involved*. Indeed, the prediction that the component of the sea arising from the long-range piece of the pion cloud of the nucleon satisfies $\bar{d} : \bar{u} = 5:1$ is totally consistent with charge independence. Thus the violation of the Gottfried sum rule and the subsequent measurement of $\bar{d} - \bar{u}$ gives us direct evidence that there is a sizable non-perturbative component of the nucleon sea. Various studies of the pion cloud of the nucleon since the original NMC measurement¹⁴ have concluded that this is indeed the most likely explanation of the observed violation of the sum rule^{15,16,17,18,19}.

In Fig.1 we show the calculated ratio of \bar{d}/\bar{u} from the πN Fock component of the nucleon wave function as a source of asymmetry, in comparison with the data points extracted from the preliminary results³ from the E866 collaboration on the ratio of pD and pp Drell-Yan cross sections. The calculation was performed in the light-cone formalism^{20,21} with a monopole πNN form factor mass parameter $\Lambda = 0.7, 1.0$ and 1.3 GeV — from smallest to largest. Clearly the agreement is qualitatively excellent, but a more detailed analysis needs to be carried out once all the data have been analysed. Let us emphasise once more the importance of these data, which are giving us direct insight into the way dynamical chiral symmetry breaking is realized in the nucleon.

3 Intrinsic strangeness and charm

The experience with the breaking of $SU(2)_F$ symmetry, which we have just described, leads us to take much more seriously the possibility of an intrinsic component of the strange and charm quark sea. The former was first discussed by Signal and Thomas²² and has recently been investigated by a number of authors^{23,24} in the light of new neutrino data from CCFR²⁵. The implication of a non-perturbatively generated component of the strange sea is a marked asymmetry between s and \bar{s} , which will clearly be the subject of much more detailed investigation in future.

With regard to the question of intrinsic charm, there has been some suggestion that it may play a role in the anomalous events seen recently at HERA – see section 5 below. For example, Gunion and Vogt²⁶ examined a model of the 5-quark component of the nucleon wave function on the light-cone²⁷. Following Brodsky *et al.*²⁷, the wave function was assumed to be inversely proportional to the light-cone energy difference between the nucleon ground state and the 5-quark excited state. The resulting x -dependence of the inclusive c quark distribution in the minimal model of²⁶ was given by²⁷:

$$\delta^{(IC)}c(x) = 6x^2 \left((1-x)(1+10x+x^2) - 6x(1+x) \log 1/x \right), \quad (1)$$

with the normalization fixed to 1%. Such a distribution peaks at $x \sim 0.2$, and is negligible beyond $x \sim 0.7$. The anti-charm distribution is assumed to be equal to the charm distribution in this model, $\delta^{(IC)}\bar{c}(x) = \delta^{(IC)}c(x)$.

As an alternative to the intrinsic charm picture of Refs.^{26,27}, in Refs.^{28,29} the charmed sea was taken to arise from the quantum fluctuation of the nucleon to a virtual $D\Lambda_c$ configuration – by analogy with the successful description of the observed $\bar{d} - \bar{u}$ asymmetry in the light-quark sector. The nucleon charm radius²⁸ and the charm quark distribution²⁹ were both estimated in this framework. Whether the same philosophy can be justified for a cloud of heavy charmed mesons and baryons around the nucleon is rather more questionable given the large mass of the fluctuation. Nevertheless, to a first approximation, we may take the meson cloud framework as an indicator of the possible shape of the non-perturbative charm distribution. A natural prediction of this model are highly asymmetric c and \bar{c} distributions.

In the meson cloud model, the distribution of charm quarks in the nucleon on the light cone at some low hadronic scale is written in convolution form³¹:

$$\delta\bar{c}(x) = \int_x^1 \frac{dz}{z} f_{D/N}(z) \bar{c}^D\left(\frac{x}{z}\right), \quad \delta c(x) = \int_x^1 \frac{dz}{z} f_{\Lambda_c/N}(z) c^{\Lambda_c}\left(\frac{x}{z}\right), \quad (2)$$

where z is the fraction of the nucleon's light-cone momentum carried by the D meson or Λ_c . The light cone (or infinite momentum frame) distribution of D

mesons in the nucleon is given by:

$$f_{D/N}(z) = \int_0^\infty \frac{dk_\perp^2}{16\pi^2} \frac{g^2(k_\perp^2, z)}{z(1-z)(s_{D\Lambda_c} - M_N^2)^2} \left(\frac{k_\perp^2 + [M_{\Lambda_c} - (1-z)M_N]^2}{1-z} \right), \quad (3)$$

and can be shown to be related to the light-cone distribution of Λ_c baryons, $f_{\Lambda_c/N}(z)$, by $f_{\Lambda_c/N}(z) = f_{D/N}(1-z)$. In Eq.(3) the function g describes the extended nature of the $D\Lambda_c N$ vertex, with the momentum dependence parameterized by $g^2(k_\perp^2, z) = g_0^2 (\Lambda^2 + M_N^2)/(\Lambda^2 + s_{D\Lambda_c})$, where the $D\Lambda_c$ center of mass energy squared is given by $s_{D\Lambda_c} = (k_\perp^2 + M_D^2)/z + (k_\perp^2 + M_{\Lambda_c}^2)/(1-z)$, and g_0 is the $D\Lambda_c N$ coupling constant at the pole, $s_{D\Lambda_c} = M_N^2$. We expect g_0 to be similar to the πNN coupling constant.

Because of the large mass of the c quark, one can approximate the \bar{c} distribution in the D meson²⁹ and the c distribution in the Λ_c by:

$$\bar{c}^D(x) \approx \delta(x-1), \quad c^{\Lambda_c}(x) \approx \delta(x-2/3), \quad (4)$$

which then gives:

$$\delta\bar{c}(x) \approx f_{D/N}(x), \quad \delta c(x) \approx \frac{3}{2}f_{\Lambda_c/N}(3x/2). \quad (5)$$

The resulting δc and $\delta\bar{c}$ distributions are shown in Fig.2, calculated for an ultraviolet cutoff of $\Lambda \approx 2.2$ GeV, which gives $\int_0^1 dx \delta c(x) = \int_0^1 dx \delta\bar{c}(x) \approx 1\%$. For a probability of 0.5% one would need a smaller cutoff, $\Lambda \approx 1.7$ GeV. Quite interestingly, the shape of the c quark distributions is similar to that in the intrinsic charm model of Refs.^{26,27}. However, as mentioned above, the model of^{26,27} assumes identical shapes for the non-perturbative c and \bar{c} distributions, while the meson cloud gives a significantly harder \bar{c} distribution. It is a very important issue for our understanding of strong interaction dynamics whether or not the charm quark distributions exhibit such an asymmetry.

4 The role of perturbative QCD at large- x

The precise mechanism whereby the SU(6), spin-flavor symmetry of the parton distributions of the nucleon is broken is a question of fundamental importance in hadronic physics. The SU(6) spin-flavour wave function of a proton, polarized in the $+z$ direction, has the form³²:

$$\begin{aligned} |p \uparrow\rangle = & \frac{1}{\sqrt{2}} |u \uparrow (ud)_{S=0}\rangle + \frac{1}{\sqrt{18}} |u \uparrow (ud)_{S=1}\rangle - \frac{1}{3} |u \downarrow (ud)_{S=1}\rangle \\ & - \frac{1}{3} |d \uparrow (uu)_{S=1}\rangle - \frac{\sqrt{2}}{3} |d \downarrow (uu)_{S=1}\rangle, \end{aligned} \quad (6)$$

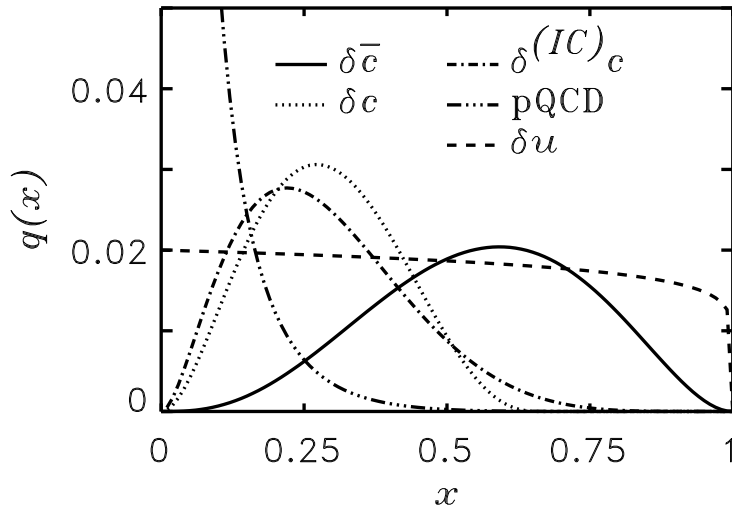


Figure 2: The non-perturbative δc and $\delta \bar{c}$ distributions in the meson cloud model³¹ (the latter normalized to 1%). Also shown is the light-cone intrinsic charm distribution, $\delta^{(IC)}_c$, of Refs.^{26,27} and the modification δu of the valence u distribution from Ref.³⁰. The purely perturbative contribution at $Q^2 = 4 \text{ GeV}^2$ is also shown.

For the neutron to proton structure function ratio this implies:

$$\frac{F_2^n}{F_2^p} = \frac{2}{3} \quad ; \quad \text{SU(6) symmetry.} \quad (7)$$

Of course, SU(6) spin-flavor symmetry is not exact. The nucleon and Δ masses are split by some 300 MeV and empirically the d quark distribution is softer than the u . The correlation between the mass splitting in the **56** baryons and the large- x behavior of F_2^n/F_2^p was observed some time ago by Close³³ and Carlitz³⁴. Based on phenomenological arguments, the breaking of the symmetry in Eq.(6) was argued to arise from a suppression of the “diquark” configurations having $S = 1$ relative to the $S = 0$ configuration. Such a suppression is, in fact, quite natural if one observes that whatever mechanism leads to the observed $N - \Delta$ splitting (e.g. color-magnetic force, instanton-induced interaction, pion exchange), necessarily acts to produce a mass splitting between the possible spin states of the spectator pair, $(qq)_S$, with the $S = 1$ state

heavier than the $S = 0$ state by some 200 MeV³⁵. From Eq.(6), a dominant scalar valence diquark component of the proton suggests that in the $x \rightarrow 1$ limit F_2^p is essentially given by a single quark distribution (i.e. the u), in which case:

$$\frac{F_2^n}{F_2^p} \rightarrow \frac{1}{4}, \quad \frac{d}{u} \rightarrow 0 \quad ; \quad S = 0 \text{ dominance.} \quad (8)$$

This expectation has, in fact, been built into all phenomenological fits to the parton distribution data.

An alternative suggestion, based on perturbative QCD, was originally formulated by Farrar and Jackson³⁶. There it was argued that the exchange of longitudinal gluons, which are the only type permitted when the spin projections of the two quarks in $(qq)_S$ are aligned, would introduce a factor $(1-x)^{1/2}$ into the Compton amplitude — in comparison with the exchange of a transverse gluon between quarks with spins anti-aligned. In this approach the relevant component of the proton valence wave function at large x is that associated with states in which the total “diquark” spin *projection*, S_z , is zero. Consequently, scattering from a quark polarized in the opposite direction to the proton polarization is suppressed by a factor $(1-x)$ relative to the helicity-aligned configuration.

A similar result is also obtained in the treatment of Brodsky *et al.*³⁷ (based on counting-rules), where the large- x behavior of the parton distribution for a quark polarized parallel ($\Delta S_z = 1$) or antiparallel ($\Delta S_z = 0$) to the proton helicity is given by: $q^{\uparrow\downarrow}(x) = (1-x)^{2n-1+\Delta S_z}$, where n is the minimum number of non-interacting quarks (equal to 2 for the valence quark distributions). In the $x \rightarrow 1$ limit these arguments, based on PQCD, suggest:

$$\frac{F_2^n}{F_2^p} \rightarrow \frac{3}{7}, \quad \frac{d}{u} \rightarrow \frac{1}{5} \quad ; \quad S_z = 0 \text{ dominance.} \quad (9)$$

Note that the d/u ratio *does not vanish* in this case. Clearly, if one is to understand the dynamics of the nucleon’s quark distributions at large x , it is imperative that the consequences of these models be tested experimentally.

5 Reanalysis of the experimental data at large- x

Information on the structure functions of the neutron is obtained from the analysis of deep-inelastic scattering data on the deuteron^{38,39}. Amongst the many approaches to this problem we mention the light-front treatment^{40,41} and the relativistic impulse approximation^{42,43}, involving the free nucleon structure function at a shifted value of x or Q^2 ^{44,45}. A more phenomenological

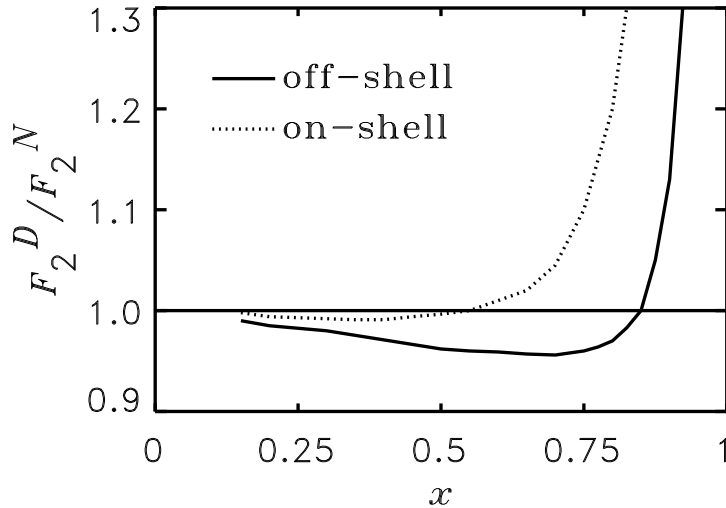


Figure 3: F_2^D/F_2^N ratio as a function of x for the model of Refs.^{49,58} (solid) which accounts for off-shell kinematics, and the on-shell model of Ref.⁴⁰ (dotted) — from Ref.⁵⁸.

approach, developed by Frankfurt and Strikman⁴⁶, attempts to derive the nuclear correction in the deuteron by extrapolation from higher A as a function of the “effective density” of the nucleus. The experimental extraction of F_2^n is usually made using either the phenomenological effective density approach or the older, “pre-EMC” theoretical treatments.

Within traditional nuclear physics the natural approach to the structure function of the deuteron is the impulse approximation. This assumes a convolution of the free nucleon structure function, F_2^N , with the non-relativistic momentum distribution $f_{N/D}$ of nucleons in the deuteron, calculated in terms of a non-relativistic wave function of the deuteron and its binding energy. Although the binding energy is very small, the kinetic energy of the recoiling nucleon plays a significant role in forcing the struck nucleon further off-shell than one would usually expect⁴⁴.

In order to assess the theoretical reliability of the non-relativistic impulse approximation one needs to go beyond the usual assumptions made in the convolution approach⁴⁸. In particular, the ingredients necessary for a covariant,

relativistic description are a covariant DNN vertex with one of the nucleons (the spectator to the hard collision) on-mass-shell, and an off-shell photon–nucleon scattering amplitude (“off-shell nucleon structure function”) \widehat{W} , the full structure of which was only recently derived in Ref.⁴⁹.

The analysis of Ref.⁴⁹ showed that the most general form of the operator \widehat{W} (which is a 4×4 matrix in Dirac space), consistent with the discrete symmetries and gauge invariance, which contributes in the Bjorken limit is:

$$\widehat{W} = \widehat{W}_0 I + \widehat{W}_1 \not{p} + \widehat{W}_2 \not{q}, \quad (10)$$

where the \widehat{W}_i are functions of p^2, q^2 and $p \cdot q$ (q is the virtual photon four-momentum). Thus, whereas in the free case the nucleon structure function involves the combination:

$$\text{Tr}[(\not{p} + M)\widehat{W}] \sim M\widehat{W}_0 + M^2\widehat{W}_1 + p \cdot q\widehat{W}_2, \quad (11)$$

the deuteron structure function involves:

$$\text{Tr}[(A_0 + \gamma^\mu A_{1\mu})\widehat{W}] \sim A_0\widehat{W}_0 + p \cdot A_1\widehat{W}_1 + q \cdot A_1\widehat{W}_2. \quad (12)$$

Clearly then, even in the absence of Fermi motion, one finds that in general $F_2^D \neq F_2^N$.

Having established that, in principle, the structure function of the bound nucleon cannot equal the structure function of the free nucleon, the important question is how big the difference actually is in practice. To estimate this, one can construct a simple model⁴⁹ of the so-called hand-bag diagram for an off-shell nucleon, in which the N -quark vertex is taken to be either a simple scalar or pseudo-vector, with the parameters adjusted to reproduce the free nucleon structure functions⁵⁰.

The result of the fully off-shell calculation from Ref.⁵⁸ is shown in Fig.3 (solid curve), where the ratio of the total deuteron to nucleon structure functions (F_2^D/F_2^N) is plotted. (We note that the behaviour of the full off-shell curve in Fig.3. is qualitatively similar to that found by Uchiyama and Saito⁵³, Kaptari and Umnikov⁴¹, and Braun and Tokarev⁴³.) We also show the result of an on-mass-shell calculation from Ref.⁴⁰ (dotted curve), which has been used in many previous analyses of the deuteron data^{52,38}. The most striking difference between the curves is the fact that the on-shell ratio has a very much smaller trough at $x \approx 0.3$, and rises faster above unity (at $x \approx 0.5$) than the off-shell curve, which has a deeper trough, at $x \approx 0.6 - 0.7$, and rises above unity somewhat later (at $x \approx 0.8$).

Clearly, a smaller D/N ratio at large x , as in Refs.^{49,58}, implies a larger neutron structure function in this region. To estimate the size of the effect

on the n/p ratio requires one to extract F_2^n , while taking care to eliminate any effects that may arise from the extraction method itself. Melnitchouk and Thomas⁵⁵ therefore used exactly the same extraction procedure as used in previous EMC⁵² and SLAC³⁸ data analyses, namely the smearing (or deconvolution) method discussed by Bodek *et al.*⁵⁶. *This method involves the direct use of the proton and deuteron data, without making any assumption concerning F_2^n itself.*

The results of this analysis are presented in Fig.4, using both the off-shell calculation⁵⁸ (solid points) and the on-shell model⁴⁰ (open points). The increase in the ratio at large x for the off-shell case is a direct consequence of the deeper trough in the F_2^D/F_2^N ratio in Fig.3. We notice, in particular, that the values of F_2^n/F_2^p obtained with the off-shell method appear to approach a value broadly consistent with the Farrar-Jackson³⁶ prediction of $3/7$, whereas the data previously analyzed in terms of the on-shell formalism produced a ratio tending to the lower value of $1/4$.

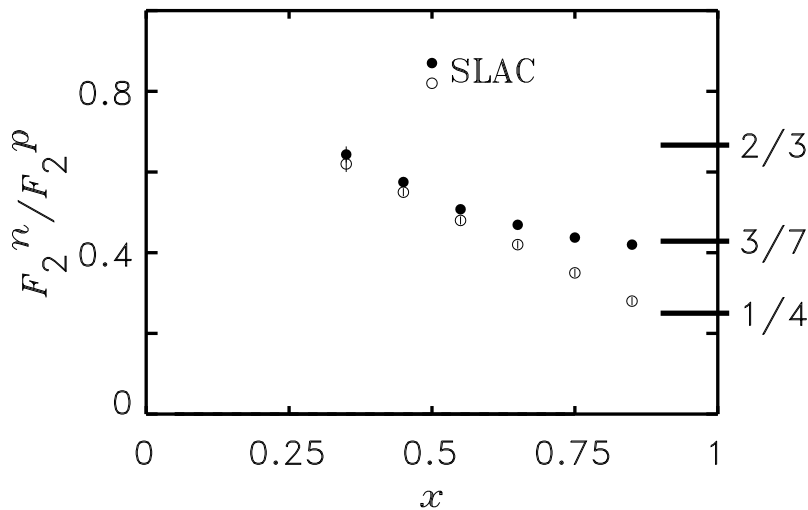


Figure 4: Deconvoluted F_2^n/F_2^p ratio extracted from the SLAC p and D data^{38,39} using the model of Ref.^{49,58} (solid circles) and Ref.⁴⁰ (open circles) – from Ref.⁵⁵.

The d/u ratio, shown in Fig.5, is obtained by inverting F_2^n/F_2^p in the

valence quark dominated region. The points extracted using the off-shell formalism (solid circles) are again significantly above those obtained previously with the aid of the on-shell prescription. In particular, they indicate that the d/u ratio may actually approach a *finite* value in the $x \rightarrow 1$ limit, contrary to the expectation of the model of Refs.^{33,34}, in which d/u tends to zero. Although it is *a priori* not clear at which scale these model predictions should be valid, for the values of Q^2 corresponding to the analyzed data the effects of Q^2 evolution are minimal.

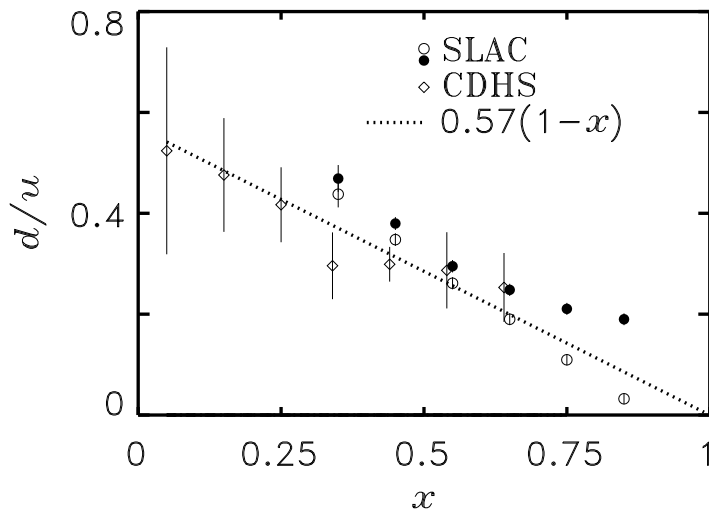


Figure 5: The d/u ratio extracted from the results of Fig.4. Also shown for comparison is the ratio extracted from neutrino measurements by the CDHS collaboration⁵⁷ and (dotted line) a standard linear fit.

Naturally, it would be preferable to extract F_2^n at large x without having to deal with uncertainties in the nuclear effects. In principle this could be achieved by using neutrino and antineutrino beams to measure the u and d distributions in the proton separately, and reconstructing F_2^n from these. Unfortunately, as seen in Fig.5, the neutrino data do not extend out to very large x ($x > 0.6$), and at present cannot discriminate between the different methods of analyzing the electron–deuteron data.

6 The HERA Anomaly

The H1 and ZEUS experiments at HERA have recently produced a small number of events at enormously high Q^2 which have generated tremendous theoretical interest^{59,60}. For $Q^2 > 10,000\text{GeV}^2$ and $x > 0.45$ the valence parton distributions are calculated to drop dramatically. The HERA anomaly is essentially the excess of observed “neutral current” (NC) events (i.e., events of the type $e^+p \rightarrow e^+X$) over expectations by roughly an order of magnitude. Many exotic explanations of this excess have already been suggested, indeed, the number of possibilities currently exceeds the number of events. However, before the new physics can be worked out one must be sure that the input parton distributions used to estimate “background” rates are reliable.

One glaring problem with the current treatment of the partonic “background” is that *all* of the standard distributions used are constructed to satisfy $d/u \rightarrow 0$ as $x \rightarrow 1$ at low- Q^2 . As we have seen, the recent re-analysis of the deuteron data leads to a d/u ratio which appears to be consistent with the prediction of PQCD that $d/u \rightarrow 1/5$ as $x \rightarrow 1$. In the light of this result it is not only vital to find alternative, more direct measurements of d/u at large x , but those generating standard sets of parton distributions should at the very least present alternative parameter sets consistent with the new analysis of the deuteron data. Until parameter sets are constructed which are consistent with $d/u \rightarrow 1/5$ as $x \rightarrow 1$, at $Q^2 \sim 10\text{ GeV}^2$, one cannot be sure of the reliability of “background” rate estimates at the extreme values of Q^2 and x being probed at HERA.

The effect of an intrinsic charm component of the sea of the nucleon was recently examined by Gunion and Vogt²⁶, with the conclusion that, as calculated on the basis of counting rules, it was too soft to explain the observed anomaly. What one needs, therefore, is a substantially harder distribution which has significantly more strength above $x \sim 0.6$ than in Eq.(1). This was precisely what was found in the non-perturbative calculation of Melnitchouk and Thomas³¹ – see Fig.2 above.

The calculation of the NC and CC cross sections requires parton distributions for all flavors. For this we use a recent parameterization of global data from the CTEQ Collaboration⁶². Expressions for the differential NC and CC cross sections $d^2\sigma/dxdQ^2$ in the standard model can be found in Refs.⁶⁰ and ⁶³. In Fig.6 we show the ratios of the modified to standard DIS model NC cross sections, with $\sigma \equiv d^2\sigma/dxdQ^2$, and $\sigma + \delta\sigma$ represents the cross section calculated with the modified distributions. The result with the modified u distribution³⁰, which was rather artificially created to reproduce the HERA anomaly, rises sharply above $M \sim 200\text{ GeV}$. The effect is rather similar if one

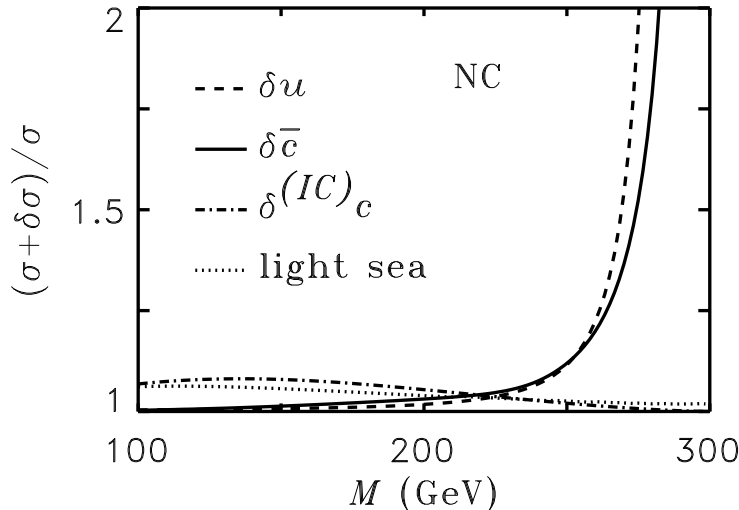


Figure 6: Ratio of modified to standard DIS model NC cross sections at the charm threshold (from Ref. ³¹), with the modifications arising from the additional u quark component ³⁰ (dashed), 1% non-perturbative $\delta\bar{c}$ and δc distributions from the meson cloud model (solid), and the intrinsic charm model of Refs.^{26,27} (dot-dashed). Also shown is the effect of the meson cloud contributions to the light sea quarks (dotted).

includes the non-perturbative δc and $\delta\bar{c}$ distributions from the meson cloud model. On the other hand, with the somewhat softer, intrinsic charm distribution of Refs. ^{26,27}, the enhancement is rather modest, and less than about 10% over the whole range of M .

We also show the effect of additional contributions to the light flavor distributions (u, \bar{u}, d and \bar{d}) which one would obtain from the pion cloud of the nucleon. Although these are considerably larger in magnitude than the δc or $\delta\bar{c}$ distributions, because they appear at small x (~ 0.1) their effect is to yield only a very small enhancement of the cross section ratio. From this figure one can conclude that the only realistic candidates for a significant enhancement of the cross section at large M are the modified valence u distribution from Ref.³⁰, and the hard charm distributions in Eq.(5).

For scattering via the CC, the effect of the additional contributions to the parton distributions is shown in Fig.7 for $Q^2 = 20000 \text{ GeV}^2$. Since the W^+

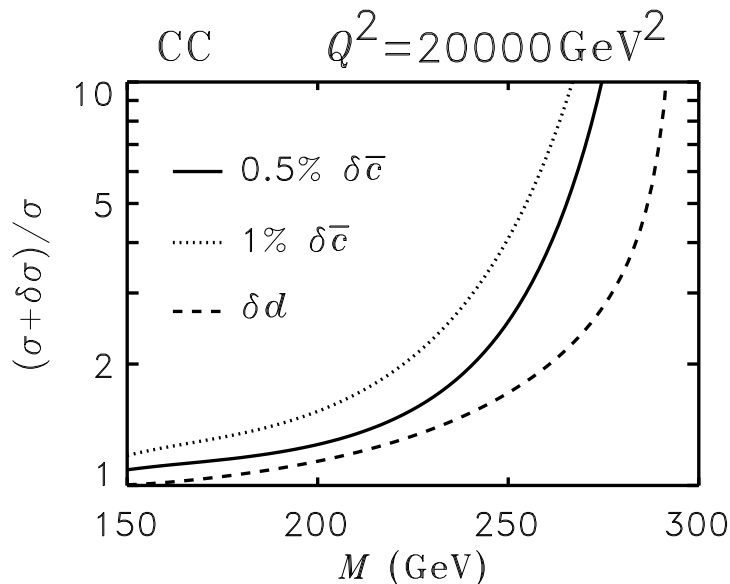


Figure 7: Ratio of modified to standard DIS model CC cross sections at $Q^2 = 20000 \text{ GeV}^2$, with the modifications arising from 0.5% and 1% additional $\delta\bar{c}$ distributions, as well as a modified d quark distribution at large x – from Ref. ³¹.

boson is not sensitive to the u quark in the proton, the δu modification has no effect on the e^+p cross section. In contrast, as noted by Babu *et al.* ⁶⁴, the effect of an additional non-perturbative $\delta\bar{c}$ contribution is an even larger enhancement of the CC cross section than the NC cross section. With a 0.5% (1%) intrinsic charm component the CC cross section increases by a factor ~ 2 (3) for $200 < M < 250 \text{ GeV}$, which is similar to the excess observed by H1 ⁵⁹ in this region.

7 Spin Dependent Structure Functions

The spin structure functions of the nucleon, $g_1^{p(n)}$, are of tremendous interest at present. Experimentally, g_1 is proportional to the difference of DIS cross sections for ep scattering with beam and target helicities aligned and anti-aligned ⁶¹. Within the parton model it may be written in terms of the parton helicity (loosely “spin”) distributions, $\Delta q(x) = [q^\uparrow - q^\downarrow + \bar{q}^\uparrow - \bar{q}^\downarrow]$, with $q^{\uparrow(\downarrow)}$ the number density of quarks with helicity parallel (anti-parallel) to the helicity of

the target proton:

$$g_1^p(x) = \frac{1}{2} \sum_q e_q^2 \Delta q(x). \quad (13)$$

Intense interest in the spin structure functions began in 1988 when EMC announced a large violation of the Ellis-Jaffe sum rule⁶⁵, which relates $\Gamma_p(Q^2) \equiv \int_0^1 g_1^p(x, Q^2) dx$ to the isovector and octet axial-vector coupling constants, $g_A^{(3)}$ and $g_A^{(8)}$. The failure of this sum rule, which is not a rigorous consequence of QCD, led to questions about the Bjorken sum rule, which relates $\Gamma_p - \Gamma_n$ to $g_A^{(3)}/6$ (modulo QCD radiative corrections⁶⁶) and *is* a strict consequence of QCD. To determine Γ_n one must measure $g_1^n(x)$, which requires a polarized nuclear target such as ^3He or D . At present, all neutron data extracted from the deuteron are obtained by applying a simple, non-relativistic prescription to correct g_1^D for the D -state component (probability ω_D) of the deuteron wave function⁶⁷:

$$g_1^n(x) = \left(1 - \frac{3}{2}\omega_D\right)^{-1} g_1^D(x) - g_1^p(x). \quad (14)$$

As we explain below, exactly the same techniques described in section 5 may be used to test the accuracy of Eq.(14).

While most interest has been focussed on the issue of sum rules, we stress that the shapes of $g_1^p(x)$ and $g_1^n(x)$ contain even more important information. For example, the same arguments that led to different conclusions about the behaviour of d/u as $x \rightarrow 1$ also give quite different predictions for g_1^p and g_1^n as $x \rightarrow 1$, namely $1/4$ and $3/7$, respectively. Quite interestingly, while the ratio of the polarized to unpolarized u quark distributions is predicted to be the same in the two models:

$$\frac{\Delta u}{u} \rightarrow 1 \quad ; \quad S = 0 \text{ or } S_z = 0 \text{ dominance}, \quad (15)$$

the results for the d -quark distribution ratio differ even in sign:

$$\frac{\Delta d}{d} \rightarrow -\frac{1}{3} \quad ; \quad S = 0 \text{ dominance}, \quad (16)$$

$$\rightarrow 1 \quad ; \quad S_z = 0 \text{ dominance}. \quad (17)$$

Using the same techniques described earlier for the unpolarized case, Melnitchouk, Piller and Thomas⁶⁸ derived the most general, antisymmetric, Dirac tensor operator of twist 2 for an off-mass-shell nucleon (see also⁶⁹):

$$\hat{G}^{\mu\nu} = i\epsilon^{\mu\nu\alpha\beta} q_\alpha \left[p_\beta (\not{p}\gamma_5 \hat{G}_p + \not{q}\gamma_5 \hat{G}_q) + \gamma_\beta \gamma_5 \hat{G}_\gamma \right]. \quad (18)$$

Once again, one finds that three functions, \hat{G}_i , can be constructed in terms of scalar and pseudo-scalar vertices. However, in this case there is a new feature, *the function \hat{G}_p does not contribute for a free nucleon*, whereas it does contribute in a nucleus.

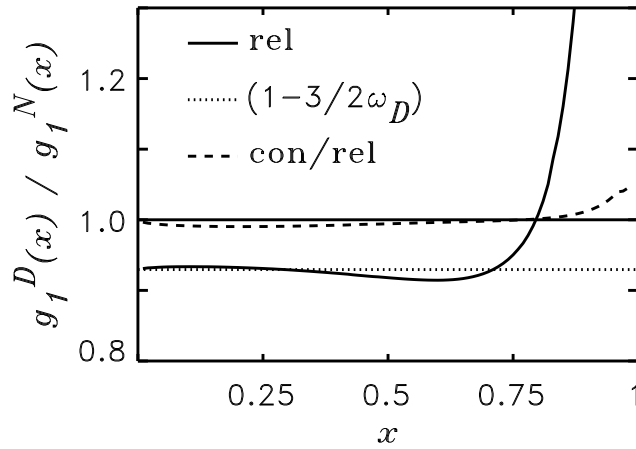


Figure 8: Ratio of deuteron and nucleon structure functions in the full model (solid), and with a constant depolarization factor corresponding to $\omega_D = 4.7\%$ (dotted line). The dashed curve is the ratio of g_1^D calculated via convolution to g_1^D calculated in the relativistic model — from Ref.⁶⁸.

The spin-dependent deuteron structure function is given by the trace of $\hat{G}^{\mu\nu}$ with a spin-dependent ND amplitude⁶⁸, which can be evaluated using the relativistic DNN vertex of Ref.⁷⁰. Surprisingly, Fig.8 shows that the ratio of the convolution approximation to the fully off-shell calculation (the dashed curve) is even closer to unity in this case than in the spin-independent case.

The comparison between the solid and dotted curves in Fig.8 shows that Eq.(14) is reliable at the 2% level for x below 0.7. However, the excellent agreement in this region between (14) and the full calculation relies on a knowledge of the deuteron D -state probability. As shown in Ref.⁶⁸, a change of ω_D by 2% (e.g. from 4% to 6%) leads to an error of order 10% or more in g_1^n . For $x > 0.7$, on the other hand, the approximation (14) fails dramatically. This will be extremely important when testing the predictions of PQCD for the $x \rightarrow 1$ behavior of the polarized distributions in Eqs.(15)–(17).

8 Conclusions

As we have seen, there is now overwhelming experimental evidence for a large, non-perturbative component of the non-strange sea of the nucleon. This is almost certainly associated with the pion cloud of the nucleon. A full, quantitative analysis of the relevant data, especially the Drell-Yan data from FNAL, will provide important new insight into the process of dynamical symmetry breaking in QCD.

Having seen the importance of the non-perturbative component of the non-strange sea, it is natural to ask about the strange and even the charm sea. For the former there is, as yet, no evidence for an asymmetry between s and \bar{s} quarks – although there are limits on how big it could be. On the other hand, in the case of charm there is tremendous interest in a possible non-perturbative component – the intrinsic charm sea. Amongst other things this is important for the interpretation of the anomaly at high invariant mass observed recently at HERA. From the theoretical point of view it is a totally open question whether or not there is an intrinsic charm sea and, if so, whether or not it is asymmetric.

The large- x region of the parton distributions corresponds to the high momentum components of the nucleon wave function. It is a vital question for our understanding of hadron structure just how these high momentum components are generated. We have seen that the most recent analysis of the structure function of the deuteron strongly supports the suggestion that these high momentum components are generated by gluon final state interactions which can be understood in terms of perturbative QCD. As a consequence the valence d/u ratio seems not to vanish as $x \rightarrow 1$. This idea needs further testing but certainly has important consequences for event rates at machines like HERA.

Our new understanding of the unpolarized parton distributions at large- x also leads us to new expectations for the polarized distributions – especially for the polarized neutron. The extraction of this information using a bound neutron target requires a sophisticated understanding of off-shell corrections in nuclear deep-inelastic scattering.

Acknowledgments

It is a pleasure to acknowledge the contributions to the work described here by W. Melnitchouk, G. Piller and A. Schreiber. I would also like to thank Prof. Dong-Pil Min and the other staff of the Asia Pacific Center for Theoretical Physics for their hospitality during this workshop, held in honour of Mannque Rho's 60th birthday. This work was supported by the Australian Research

Council.

References

1. F. X. Lee and D. B. Leinweber, hep-lat/9711044.
2. A. W. Thomas, Prog. Part. Nucl. Phys. **20** (1988) 21.
3. E.A. Hawker *et al.* (E866 Collaboration), “Measuring the $\bar{u} - \bar{d}$ Asymmetry in the Proton Sea”, presented at XXXII Moriond Conference, 22-29 March 1997.
4. A. W. Thomas and W. Melnitchouk, hep-ph/9708484.
5. T. Inoue and T. Maskawa, Prog. Theor. Phys. **54** (1975) 1833.
6. A. Chodos and C.B. Thorn, Phys. Rev. D **12** (1975) 359.
7. G.E. Brown and M. Rho, Phys. Lett. B **82** (1979) 177.
8. S. Théberge, G.A. Miller and A.W. Thomas, Phys. Rev. D **22** (1980) 2838; *ibid* D **23** (1981) 2106(e); A.W. Thomas, Adv. Nucl. Phys. **13** (1984) 1; G.A. Miller, Int. Rev. Nucl. Phys. **2** (1984) 190.
9. J.D. Sullivan, Phys. Rev. D **5** (1972) 1732.
10. C.H. Llewellyn Smith, Phys. Lett. B **128** (1983) 107.
11. M. Ericson and A.W. Thomas, Phys. Lett. B **128** (1983) 112.
12. A.W. Thomas, Phys. Lett. B **126** (1983) 97.
13. L.L. Frankfurt, L. Mankiewicz and M.I. Strikman, Zeit. Phys. A **334** (1989) 334; W. Koepf, L.L. Frankfurt and M.I. Strikman, Phys. Rev. D **53** (1996) 2586.
14. P. Amaudruz *et al.* (NMC), Phys. Lett. B **295** (1992) 159; Phys. Rev. Lett. **66** (1991) 2712.
15. J. Speth and A.W. Thomas, “Mesonic Contributions to the Spin and Flavor Structure of the Nucleon” (Jül-3283, Sept. 1996), to appear in Adv. Nucl. Phys. (1998).
16. E.M. Henley and G.A. Miller, Phys. Lett. B **251** (1990) 453.
17. A.I. Signal, A.W. Schreiber and A.W. Thomas, Mod. Phys. Lett. A **6** (1991) 271.
18. S. Kumano and J.T. Londergan, Phys. Rev. D **44** (1991) 717; S. Kumano, hep-ph/9702367.
19. W.-Y.P. Hwang, J. Speth and G.E. Brown, Zeit. Phys. A **339** (1991) 383.
20. W. Melnitchouk and A.W. Thomas, Phys. Rev. D **47** (1993) 3794.
21. V.R. Zoller, Z. Phys. C **60** (1993) 141.
22. A.I. Signal and A.W. Thomas, Phys. Lett. B **191** (1987) 205.
23. S.J. Brodsky and B.-Q. Ma, Phys. Lett. B **381** (1996) 317.
24. X. Ji and J. Tang, Phys. Lett. B **362** (1995) 182; H. Holtmann *et al.*,

- Nucl. Phys. A **569** (1996) 631; W. Melnitchouk and M. Malheiro, Phys. Rev. C **55** (1997) 431.
25. A. Bazarko *et al.* (CCFR Collaboration), Zeit. Phys. C **65** (1995) 189.
 26. J.F. Gunion and R. Vogt, UCD-97-14, LBNL-40399 [hep-ph/9706252].
 27. S.J. Brodsky, P. Hoyer, C. Peterson and N. Sakai, Phys. Lett. **93** B, 451 (1980); S.J. Brodsky, C. Peterson and N. Sakai, Phys. Rev. D **23**, 2745 (1981).
 28. F.S. Navarra, M. Nielsen, C.A.A. Nunes and M. Teixeira, Phys. Rev. D **54**, 842 (1996).
 29. S. Paiva, M. Nielsen, F.S. Navarra, F.O. Duraes and L.L. Barz, IFUSP-P-1240 [hep-ph/9610310].
 30. S. Kuhlmann, H.L. Lai and W.K. Tung, Phys. Lett. B **409** (1997) 271.
 31. W. Melnitchouk and A.W. Thomas, hep-ph/9707387.
 32. F.E. Close, *An Introduction to Quarks and Partons* (Academic Press, 1979).
 33. F.E. Close, Phys. Lett. B **43** (1973) 422.
 34. R. Carlitz, Phys. Lett. B **58** (1975) 345.
 35. F.E. Close and A.W. Thomas, Phys. Lett. B **212** (1988) 227.
 36. G.R. Farrar and D.R. Jackson, Phys. Rev. Lett. **35** (1975) 1416.
 37. S.J. Brodsky, M. Burkardt and I. Schmidt, Nucl. Phys. **B441** (1995) 197.
 38. L.W. Whitlow *et al.*, Phys. Lett. B **282** (1992) 475.
 39. J. Gomez *et al.*, Phys. Rev. D **49** (1994) 4348.
 40. L.L. Frankfurt and M.I. Strikman, Phys. Lett. B **76** (1978) 333; Phys. Rep. **76** (1981) 215.
 41. L.P. Kaptari and A.Yu. Umnikov, Phys. Lett. B **259** (1991) 155.
 42. F. Gross and S. Liuti, Phys. Rev. C **45** (1992) 1374;
 43. M.A. Braun and M.V. Tokarev, Phys. Lett. B **320** (1994) 381.
 44. G.V. Dunne and A.W. Thomas, Nucl. Phys. A **455** (1986) 701.
 45. K. Nakano and S.S.M. Wong, Nucl. Phys. A **530** (1991) 555.
 46. L.L. Frankfurt and M.I. Strikman, Phys. Rep. **160** (1988) 235.
 47. H. Jung and G.A. Miller, Phys. Lett. B **200** (1988) 351.
 48. R.L. Jaffe, in *Relativistic Dynamics and Quark-Nuclear Physics*, eds. M.B. Johnson and A. Pickleseimer (Wiley, New York, 1985). S.V. Akulinichev, S.A. Kulagin and G.M. Vagradov, Phys. Lett. B **158** (1985) 485; S.A. Kulagin, G. Piller and W. Weise, Phys. Rev. C **50** (1994) 1154.
 49. W. Melnitchouk, A.W. Schreiber and A.W. Thomas, Phys. Rev. D **49** (1994) 1183.
 50. P. Mulders, A.W. Schreiber and H. Meyer, Nucl. Phys. A **549** (1992)

498.

- 51. W. Melnitchouk, A.W. Schreiber and A.W. Thomas, Phys. Lett. B **335** (1994) 11.
- 52. European Muon Collaboration, J.J. Aubert *et al.*, Phys. Lett. B **110** (1982) 73; Nucl. Phys. B **213** (1983) 213.
- 53. T. Uchiyama and K. Saito, Phys. Rev. C **38** (1988) 2245.
- 54. J. Carbonell, B. Desplanques, V.A. Karmanov and J.-F. Mathiot, to appear in Phys. Rep.
- 55. W. Melnitchouk and A.W. Thomas, Phys. Lett. B **377** (1996) 11.
- 56. A. Bodek *et al.*, Phys. Rev. D **20** (1979) 1471; A. Bodek and J.L. Ritchie, Phys. Rev. D **23** (1981) 1070.
- 57. H. Abramowicz *et al.* (CDHS Collaboration), Z. Phys. C **25** (1983) 29.
- 58. W. Melnitchouk, A.W. Schreiber and A.W. Thomas, Phys. Lett. B **335** (1994) 11.
- 59. C. Adloff *et al.* (H1 Collaboration), Zeit. Phys. C **74** (1997) 191.
- 60. J. Breitwig *et al.* (ZEUS Collaboration), Zeit. Phys. C **74** (1997) 207.
- 61. H.-Y. Cheng, Int. J. Mod. Phys. A **11** (1996) 5109; M. Anselmino *et al.*, Phys. Rep. **261** (1995) 1.
- 62. H.L. Lai, J. Huston, S. Kuhlmann, F. Olness, J.F. Owens, D. Soper, W.K. Tung and H. Weerts, Phys. Rev. D **55**, 1280 (1997).
- 63. H1 Collaboration, S. Aid *et al.*, Phys. Lett. B **379**, 319 (1996).
- 64. K.S. Babu, C. Kolda and J. March-Russell, Phys. Lett. B **408** (1997) 268.
- 65. J. Ashman *et al.* (EMC), Phys. Lett. B **206** (1988) 364.
- 66. S.A. Larin, T. van Ritbergen and J.A.M. Vermaseren, Phys. Lett. B **404** (1997) 153.
- 67. D. Adams *et al.* (SMC), Phys. Lett. B **357** (1995) 248; K. Abe *et al.* (E143 Collaboration), Phys. Rev. Lett. **75** (1995) 25.
- 68. W. Melnitchouk, G. Piller and A.W. Thomas, Phys. Lett. B **346** (1995) 165; G. Piller, W. Melnitchouk and A.W. Thomas, Phys. Rev. C **54** (1996) 894.
- 69. S.A. Kulagin, W. Melnitchouk, G. Piller and W. Weise, Phys. Rev. C **52** (1995) 932.
- 70. W.W. Buck and F. Gross, Phys. Rev. D **20** (1979) 2361; R.G. Arnold, C.E. Carlson and F. Gross, Phys. Rev. C **21** (1980) 1426; F. Gross, J.W. Van Orden and K. Holinde, Phys. Rev. C **45** (1992) 2094.